



# Catalytic purification of H<sub>2</sub>-rich streams by CO-PROX over Pt-Co-Ce/ $\gamma$ -Al<sub>2</sub>O<sub>3</sub> in fluidized bed reactors

M.P. Lobera, C. Téllez\*, J. Herguido, M. Menéndez

Aragón Institute of Engineering Research (I3A), Universidad de Zaragoza, 50018 Zaragoza, Spain

## ARTICLE INFO

### Article history:

Available online 26 February 2010

### Keywords:

CO-PROX

SELOX

Fluidized bed reactors

Hydrogen purification

Pt-Co-Ce/ $\gamma$ -Al<sub>2</sub>O<sub>3</sub>

## ABSTRACT

Pt-Co-Ce/ $\gamma$ -Al<sub>2</sub>O<sub>3</sub> catalyst has been prepared by incipient impregnation and tested in the preferential oxidation of CO in a H<sub>2</sub>-rich stream. Fluidized bed reactors with the reactants fed at two different points have been used in order to improve the reactants contact mode. The influence of temperature, oxygen excess ( $\lambda = 2Q_{O_2}/Q_{CO}$ ) and presence of CO<sub>2</sub> and water have been studied. The use of a two-zone fluidized bed reactor (TZFBR) allowed to optimize the oxidation state of the catalyst and obtain an effluent with a CO concentration of less than 10 ppm with a high selectivity (~77%) to the selective CO oxidation. This can be achieved without catalyst deactivation working only with a slight excess of oxygen ( $\lambda = 1.3$ ) and operating at temperatures lower than 100 °C. A conventional fluidized bed reactor requires  $\lambda$  values higher than 1.5 to achieve CO concentration of less than 10 ppm.

© 2010 Elsevier B.V. All rights reserved.

## 1. Introduction

Proton-exchange membrane fuel cells (PEMFCs) appear to be the most suitable and commercially viable hydrogen-based fuel cell systems for static and mobile applications [1]. Hydrogen is usually produced by several processes that include steam reforming, autothermal reforming or partial oxidation of natural gas, light hydrocarbons or alcohols. The gas stream obtained after these processes still contains significant amounts of CO (0.5–2% CO). Unfortunately, suitable operation in a PEMFC can only be ensured with a content of CO below 1–100 ppm, because CO is known to poison the Pt electrodes [2].

In recent years there has been a growing interest in the development of catalysts for the preferential oxidation of CO (CO-PROX). Different catalysts [2] have been developed such as metal oxides (CoO<sub>x</sub>, CuO–CeO<sub>2</sub>), supported gold catalysts, and supported noble metal (Ru, Pt, and Rh) catalysts. Fixed bed reactors are commonly used but other kinds of reactors (e.g. monolith [3,4] and membrane reactors [5,6]) have been tested and work still needs to be done on the mode of contact between reactives.

CeO<sub>2</sub> is capable of storing O<sub>2</sub> and reacts in the absence of gas phase oxygen [2]. When platinum catalysts contain reducible oxides such as cerium or cobalt, the kinetics of the CO-PROX reaction can be explained by a non-competitive Langmuir–

Hinshelwood mechanism with two types of active sites. CO adsorbed on the platinum surface reacts with oxygen atoms which are first dissociatively adsorbed on the support surface and then spilled over the Pt particle. Moreover, this reaction can occur on the metal/oxide interface and in this case is selective to CO oxidation [2,7]. This redox performance fits the mode of operation of a two-zone fluidized bed reactor (TZFBR) (Fig. 1), in which the catalyst is moving continuously between two zones created by feeding the reactants at two different points of a fluidized bed reactor. The characteristics and several applications of the TZFBR have been described previously [8]. The use of the TZFBR allows different ways of feeding the reagents creating two zones in the reactor with different characteristics depending on the configuration used. The aim of this work is to optimize the preferential oxidation of CO over a Pt-Co-Ce/ $\gamma$ -Al<sub>2</sub>O<sub>3</sub> catalyst using different fluidized bed reactor configurations (Fig. 1), in order to improve the mode of contact between reactives.

## 2. Experimental

### 2.1. Catalyst preparation and characterization

The Pt-Co-Ce/ $\gamma$ -Al<sub>2</sub>O<sub>3</sub> catalyst was prepared by incipient wet co-impregnation [9] and the nominal composition was 1.4 wt.% of Pt, 1.25 wt.% of Co and 1.25 wt.% of Ce. The support ( $\gamma$ -alumina, Puralox Sasol Germany GmbH, particle size 160–250  $\mu$ m) was calcined at 450 °C for 2 h prior to impregnation. At room temperature, aqueous solutions of Pt(NH<sub>3</sub>)<sub>4</sub>(NO<sub>3</sub>)<sub>2</sub> (Sigma–Aldrich,  $\geq 50.0\%$  Pt basis), Co(NO<sub>3</sub>)<sub>2</sub>·6H<sub>2</sub>O (Sigma–Aldrich, 98% purity) and Ce(NO<sub>3</sub>)<sub>3</sub>·6H<sub>2</sub>O (Sigma–Aldrich, 99% purity) were dripped into a

\* Corresponding author at: Chemical and Environmental Engineering Department, Universidad de Zaragoza, Centro Politécnico Superior, c/María de Luna, 3, 50018 Zaragoza, Spain. Tel.: +34 976 762471; fax: +34 976 761879.

E-mail address: [ctellez@unizar.es](mailto:ctellez@unizar.es) (C. Téllez).

## Nomenclature

|           |  |
|-----------|--|
| FBR       | fluidized bed reactor  |
| $h$       | bed height [cm]  |
| $h_a$     | intermediate feeding height [cm]   |
| $H$       | total bed length [cm]  |
| $Q_{O_2}$ | total oxygen flow rate [ $\text{cm}^3$ (STP) $\text{min}^{-1}$ ]                     |
| $Q_{CO}$  | total CO flow rate [ $\text{cm}^3$ (STP) $\text{min}^{-1}$ ]                         |
| $Q_T$     | total gases flow rate [ $\text{cm}^3$ (STP) $\text{min}^{-1}$ ]                      |
| $T$       | reaction temperature [ $^{\circ}\text{C}$ ]  |
| TZFBR     | two-zone fluidized bed reactor   |
| $u_o$     | superficial gas velocity [ $\text{cm}^3$ (STP) $\text{cm}^{-2} \text{s}^{-1}$ ]      |
| $u_{mf}$  | minimum fluidization velocity [ $\text{cm}^3$ (STP) $\text{cm}^{-2} \text{s}^{-1}$ ] |
| $u_r$     | relative gas velocity [ $u_o/u_{mf}$ ]   |
| $u_{r1}$  | relative gas velocity in reaction zone [ $u_o$ reaction zone/<br>$u_{mf}$ ]          |
| $W_r$     | catalyst weight where the CO oxidation happens [g]                                   |
| $W_T$     | catalyst weight in the reactor [g]   |

## Superscripts

|     |                         |
|-----|-------------------------|
| in  | at the reactor entrance |
| out | at the reactor exit     |

## Greek letters

|           |   |
|-----------|---|
| $\lambda$ | oxygen excess ( $\lambda = 2Q_{O_2}/Q_{CO}$ ) |
| $\xi$     | fraction of oxygen co-fed with $H_2$          |

flask at a rate of  $5 \text{ cm}^3/\text{min}$ . During the impregnation, the slurry was mixed by an ultrasonic mixer for 90 min in order to maintain a uniform distribution of the precursor solution; it was then dried in air at  $85^{\circ}\text{C}$  during 16 h. Finally, the dried catalyst was heated ( $3^{\circ}\text{C}/\text{min}$ ) to  $450^{\circ}\text{C}$  in air and calcined for 2 h. The catalyst had a minimum fluidization velocity ( $u_{mf}$ ) of  $1.44 \text{ cm}^3$  (STP)/ $\text{cm}^2$  s obtained with Ar at  $120^{\circ}\text{C}$ .

Catalyst activation was required before performing the CO-PROX experiments. The active species of platinum is  $\text{Pt}^0$ , and this requires a reduction treatment [9–12]. However, when there are transition metals such as cobalt or oxides with redox properties such as cerium oxide, an oxidation step may also be required [13]. In this study, the activation procedure consists of a reduction step (3 h at  $375^{\circ}\text{C}$ , gas mixture:  $1:1 = H_2:\text{Ar}$ ), followed by partial oxidation of the catalyst (0.5 h at  $80^{\circ}\text{C}$ , gas mixture:  $1:1 = O_2:\text{Ar}$ ). A stable catalyst has been obtained after three cycles; each cycle being composed of three steps: reduction, oxidation and reaction. In this stabilization process, the reaction is at  $90^{\circ}\text{C}$  for 6 h using a mixture 1% CO, 0.55%  $O_2$ , 60%  $H_2$  and argon to balance. This stabilization process gives a relative error lower than 0.35 for conversion and oxygen selectivity to  $CO_2$  (as is defined below). The stable catalyst is used for the performance analysis in the conventional fluidized bed reactor (FBR) and the TZFBR. In the following sections, all the results reported correspond to those obtained at a time on stream of 2 h, once steady state has been reached.

The surface area was obtained by the Brunauer–Emmet–Teller (BET) method with an automatic analyzer ASAP 2002 from Micromeritics. The commercial  $\gamma$ -alumina has a BET surface area of  $193 \text{ m}^2/\text{g}$ ; after calcinations, a  $185 \text{ m}^2/\text{g}$  solid catalyst was obtained. Thus, the BET area was maintained after metal impregnation and catalyst stabilization.

The powder X-ray diffraction (XRD) patterns were measured in a Rigaku/Max diffractometer equipped with a graphite monochro-

mator operating at 40 kV and 80 mA and using nickel-filtered  $\text{CuK}\alpha$  radiation  $1.2$  ( $2\theta = 10\text{--}90^{\circ}$ ). The “JCPDS-International Centre for Diffraction Data-2000” database has been used for the determination of the phases. As can be seen in Fig. 2, the stable and aged catalysts (250 h under operating conditions) showed clearly the broad diffraction peaks of  $\gamma\text{-Al}_2\text{O}_3$ . The  $\text{Ce}_2\text{O}_3$ ,  $\text{CeO}_2$  and  $\text{Co}_3\text{O}_4$  diffraction peaks can be hardly distinguished. Diffraction peaks of Pt have not been identified; this could indicate that the preparation method allows us to obtain small metal crystallites. The XRD results also show that the catalyst structure do not change for a long time (250 h) under the operating conditions, which is essential for achieving an active catalyst for the CO-PROX reaction [10].

A temperature-programmed reduction (TPR) experiment (not shown) was performed over a sample of stable catalyst with  $10 \text{ mL(STP)}/\text{min}$  of a  $\text{Ar:H}_2$  (95:5) mixture. A wide reduction peak was found with a maximum at around  $200^{\circ}\text{C}$ . This peak is associated with the reduction of platinum [10] and the presence of cobalt could modify the reduction temperature of the Ce oxides, and the reduction of  $\text{Ce}^{4+}$  to  $\text{Ce}^{3+}$  could be masked at that temperature [14]. Two smaller peaks also appear, one at  $425^{\circ}\text{C}$  and another at around  $720^{\circ}\text{C}$ , both associated with the reduction of cobalt [14–16].

## 2.2. Reactor setup and calculations

The catalytic oxidation of CO from a  $H_2$ -rich stream was carried out in different fluidized bed reactors (Fig. 1). The reactor was heated by an electric furnace and the temperature was measured by a thermocouple at the centre of the catalyst bed. A PID controller maintained temperature variations within  $\pm 0.5^{\circ}\text{C}$  of the set point. The reactor was a 30-mm-i.d., 300-mm-long quartz tube equipped with a sintered quartz distributor plate and a movable axial quartz probe was used to introduce gas feed at different reactor heights ( $h_a$ ).

Thus, different ways of feeding the reagents were studied, resulting in different TZFBR configurations (Fig. 1). The variation was in the mode of feeding each reactant, creating two zones in the reactor with different redox atmospheres. In configuration C-1 (Fig. 1), the mixture ( $H_2 + \text{CO}$ ) was fed to the lower part of the reactor mixed with inert gas, and  $O_2 + \text{inert gas}$  were fed at an intermediate point of the bed ( $h_a$ ) while in the configuration C-2, these gas stream was fed in contrary way. In the configurations C-3 and C-4, the ( $H_2 + \text{CO}$ ) and  $O_2$  were co-fed. Moreover, it is possible to move from the C-1 to the C-4 or from the C-2 to the C-3 configurations of the TZFBR, i.e., by changing the fraction of oxygen that is co-fed ( $\xi$ ) at an intermediate point ( $h_a$ ) of the catalyst bed (Fig. 1).

The reaction products were analyzed by online gas chromatography (Agilent 3000  $\mu\text{GC}$  equipped with a TCD detector and He as a carrier gas) and mass spectrometry (Omnistar GSD 301T). The CO calibration was made using two standard gas mixtures provided by Praxair S.A. the first one with 100 ppm of CO and 100 ppm of  $CO_2$  (argon to balance) and the second one with 10% of CO diluted in argon. The detection limit of the  $\mu\text{GC}$  was 10 ppm of CO measured with the first standard gas mixture diluted with argon using mass flow controllers. The carbon balance closure calculated from the concentrations of CO and  $CO_2$  typically agreed to within 2%. CO conversion and oxygen selectivity to  $CO_2$  (calculated as the ratio of the desired reaction (CO oxidation) to the overall  $O_2$  consumption) were defined as follows:

$$X_{CO} (\%) = \frac{Q_{CO}^{in} - Q_{CO}^{out}}{Q_{CO}^{in}} 100 \quad (1)$$

$$S_{CO_2} (\%) = \frac{0.5(Q_{CO}^{in} - Q_{CO}^{out})}{Q_{O_2}^{in} - Q_{O_2}^{out}} 100 \quad (2)$$

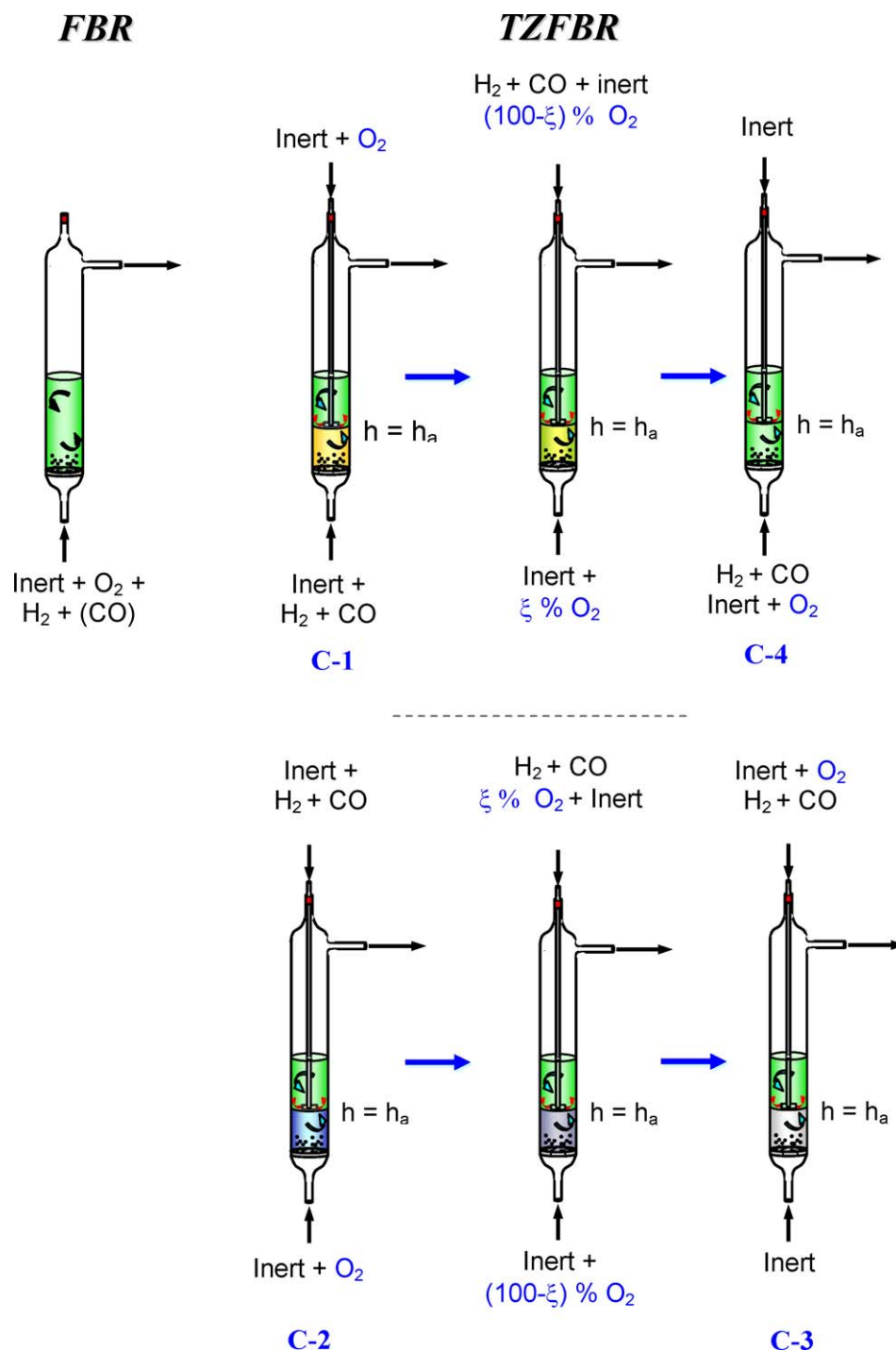


Fig. 1. Configurations of the fluidized bed reactors. Arrows inside the reactors indicate solid movement.

It should be noted that this last formula supposes that CO is exclusively converted to CO<sub>2</sub>, since methanation or coke formation reactions can be completely discarded over Pt-Co-Ce/γ-Al<sub>2</sub>O<sub>3</sub> catalyst in the temperature range studied.

The oxygen excess with respect to the amount of oxygen required for the oxidation of CO to CO<sub>2</sub> is commonly characterized by the process parameter  $\lambda$  ( $2Q_{O_2}^{in}/Q_{CO}^{in}$ ); where  $\lambda = 1$  is sufficient to provide the complete oxidation of CO to CO<sub>2</sub> in the absence of an oxygen-consuming side reaction (H<sub>2</sub> oxidation). It should be noted that in the range of operating conditions studied, the oxygen fed was completely consumed during the oxidation process.

### 3. Results

#### 3.1. Fluidized bed reactor (FBR) configuration

Fig. 3 shows the effect of the reaction temperature on CO conversion and oxygen selectivity to CO<sub>2</sub> while the other operating parameters are kept constant. From 50 °C to 90 °C, both CO conversion and the oxygen selectivity to CO<sub>2</sub> decrease sharply with the temperature. The results obtained at 40 °C were slightly lower than at 50 °C where the effluent containing less than 10 ppm of CO. This could be due to the fact that at low temperatures CO molecules

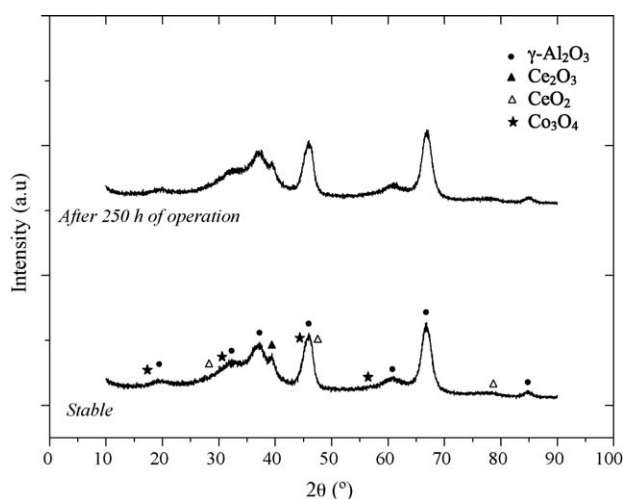


Fig. 2. XRD patterns of the stable catalyst and aged catalyst.

completely cover the Pt centers and the reaction principally takes place between adsorbed CO and oxygen atoms adsorbed on the catalyst surface, this reaction being selective for CO. The same trends have been observed by other authors for catalysts based on Pt [9–11,17]. On the other hand, when the reaction temperature increases ( $T > 80^\circ\text{C}$ ), the desorption of the CO molecules from Pt particles starts, and the adsorption of hydrogen on Pt particles is significant, so hydrogen oxidation takes place (it reacts with the active oxygen on the catalyst surface) causing a decrease in the yield of CO-PROX reaction [7,11,18]. Several studies show that the presence of cobalt in Pt-based catalysts allows relatively high conversions of CO ( $\sim 80\%$ ) to be obtained at very low temperatures [2,19].

Experiments with different amounts of oxygen were performed while maintaining constant CO and  $\text{H}_2$  total flows in the feed, the reaction temperature and the catalyst weight. In Fig. 4, CO conversion increases when the excess of oxygen increases whereas the oxygen selectivity to  $\text{CO}_2$  decreases, in agreement with the findings of other authors [7,9,17,20]. Thus the CO-PROX reaction, like most oxidation reactions, is favored as the oxygen concentration in the inlet flow increases. Nevertheless, as has been commented above, the existence of hydrogen oxidation (a parallel reaction to CO oxidation) implies that the  $\lambda$  value must be as low as

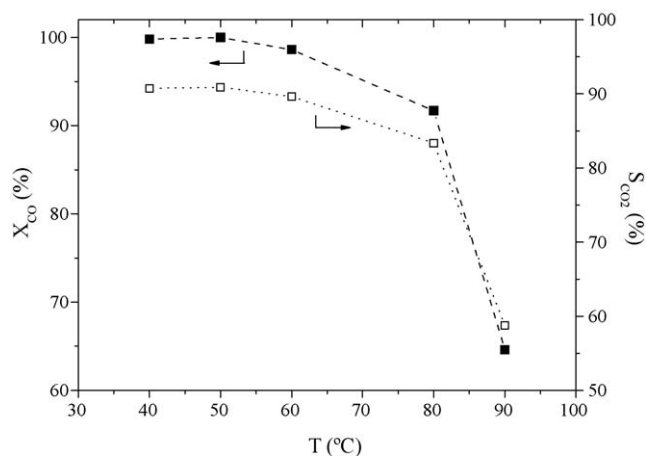


Fig. 3. Effect of reaction temperature on CO conversion and oxygen selectivity to  $\text{CO}_2$  for the PROX reaction in a FBR. 1% CO, 60%  $\text{H}_2$ ,  $\lambda = 1.1$ ,  $u_r = 2$ ,  $W_{\text{cat}} = 20$  g (symbols are experimental data and the lines are a guide for eyes).

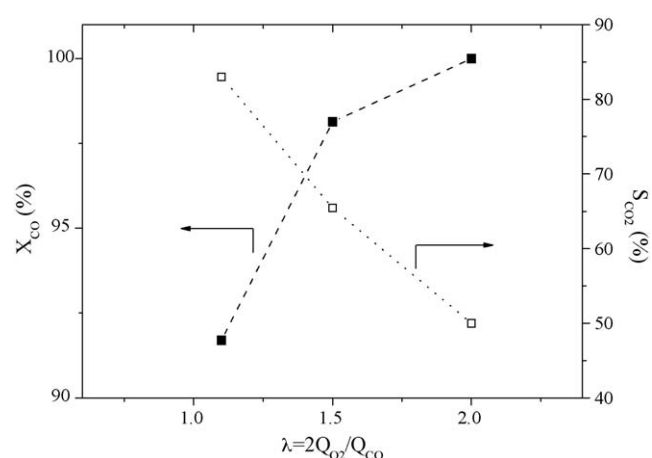


Fig. 4. CO conversion and oxygen selectivity to  $\text{CO}_2$  for the PROX reaction in a FBR as a function of oxygen excess ( $\lambda$ ).  $T = 80^\circ\text{C}$ , 1% CO, 60%  $\text{H}_2$ ,  $u_r = 2$ ,  $W_{\text{cat}} = 20$  g (symbols are experimental data and the lines are guide for eyes).

possible to obtain almost full CO conversion and the highest oxygen selectivity to  $\text{CO}_2$ . The values of  $\lambda$  that can eliminate completely the CO ( $< 10$  ppm in the exit stream) of the inlet flow are lower than those used for other catalysts based on Pt, due to the use of reducible compounds of cerium or cobalt that are capable of storing oxygen, which could react more efficiently with the CO at low  $\lambda$  values [7,9,14].

The influence of  $\text{H}_2\text{O}$  and  $\text{CO}_2$  molecules on conversion and selectivity is one of the most studied phenomena in the CO-PROX reaction because these two molecules appear together with  $\text{H}_2$  and CO in the reformed gas. Generally, and depending on the characteristics of the support, these molecules can adsorb on the active sites of the catalyst, inhibiting its activity. Numerous scientific works describe the effect that these molecules have in the catalytic behavior of this reaction [9,11,12,17,21,22], although with different conclusions. Several studies report that the presence of  $\text{CO}_2$  negatively affects the catalyst stability due to the formation of carbonates on its surface [9,12,17]. Other works report that the  $\text{CO}_2$  partial pressure does not significantly affect the  $\text{CO}_2$  production rate [22–24] and other authors observe an increase in the oxygen selectivity to  $\text{CO}_2$  [22].

Fig. 5 shows the evolution of CO conversion with the time on stream in the presence of  $\text{CO}_2$  and  $\text{CO}_2 + \text{H}_2\text{O}$  in the feed. The

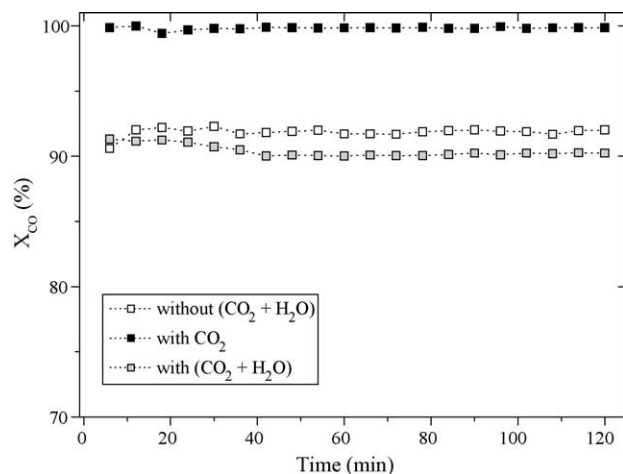


Fig. 5. Influence of  $\text{CO}_2$  and  $\text{H}_2\text{O}$  concentrations on CO conversion for the PROX reaction in a FBR as a function of time on stream.  $T = 80^\circ\text{C}$ , 1% CO, 60%  $\text{H}_2$ ,  $\lambda = 1.1$ ,  $u_r = 2$ ,  $W_{\text{cat}} = 20$  g, 20%  $\text{CO}_2$ , 1.7%  $\text{H}_2\text{O}$  (symbols are experimental data and the lines are guide for eyes).

results show that in the presence of CO<sub>2</sub>, the activity of the catalyst was notably improved, obtaining an effluent with less than 20 ppm of CO. This beneficial effect of the CO<sub>2</sub> might be due to blocking of the sites required for the hydrogen oxidation thus most of the feeding oxygen reacts to oxidize CO. However, when the test is carried out in the presence of CO<sub>2</sub> and H<sub>2</sub>O, a small decrease in CO conversion is observed compared to when these two compounds were not present in the inlet flow. Two explanations can be proposed to explain the effect of water: the presence of water could inhibit the adsorption of CO and/or CO<sub>2</sub> on the Pt particles, or water could condense inside the catalyst pores, thus the reaction is strongly influenced by mass transfer restrictions [14].

### 3.2. Operation in a two-zone fluidized bed reactor

The oxygen excess is an essential variable in the CO-PROX reaction. Its effect has therefore been studied in the operation of the different configurations of the TZFBR (Fig. 1). The experiments have been carried out varying the oxygen excess ( $\lambda$ ), but maintaining constant the reaction temperature, CO and H<sub>2</sub> concentrations in the inlet flow, the relative gas velocity ( $u_r$ ), the amount of catalyst used and the ratio of heights between the redox zones in the reactor. In the four configurations of the TZFBR studied, an increase in excess oxygen leads to an increase in CO conversion (Fig. 6) and of course a decrease in oxygen selectivity to CO<sub>2</sub> (remember O<sub>2</sub> is in all cases completely consumed), in agreement with the results obtained in the FBR configuration.

Configurations C-1 and C-2 offered worse results than the other configurations and this may be related to the absence of oxygen in the zone where the main part of the oxidation reactions occurs. Configuration C-4 allowed the highest CO conversion (a CO concentration of less than 10 ppm for  $\lambda \geq 1.5$ ), indicating that the redox state of the catalyst is more suitable than in the other configurations. In configuration C-3, the CO conversions obtained are slightly lower than those obtained in configuration C-4 because of the smaller reaction spatial time,  $W_r/Q_{CO}^{in}$ .

The use of a TZFBR allows the mixture of H<sub>2</sub> and CO and the mixture of O<sub>2</sub> and argon to be introduced at different points of the reactor. From this point of view, it is of interest to know how the CO conversion changes when the total oxygen fed to the system is distributed in two feeding zones, co-fed together with the mixture of H<sub>2</sub> and CO, or through another inlet of the TZFBR (see Fig. 1, intermediate configurations between the C-2 and C-3 configurations). Fig. 7 shows the CO conversion and oxygen selectivity to CO<sub>2</sub> by moving from the C-2 to the C-3 configuration of the TZFBR, i.e., by changing the fraction of oxygen that is co-fed ( $\xi$ ) in an intermediate point of the bed, for three different temperatures. A similar procedure has been used in a two stage packed-bed reactor, the CO conversion increasing with oxygen split [25].

For a reaction temperature of 60 °C, when the amount of O<sub>2</sub> co-fed into the reactor together with the H<sub>2</sub> increases, the CO conversion increases very slightly, although worse results are obtained when the experiment is realized with a C-3 configuration of the TZFBR. On the other hand, the effect of distributing the O<sub>2</sub> between the different feeding points is higher when the reaction temperature increases, while increasing the quantity of oxygen co-fed ( $\xi$ ) clearly gives better results. The trend with the increase of temperature is related to a greater desorption of CO adsorbed on the Pt particles so the oxidation of H<sub>2</sub> is therefore more important. Co-feeding 90% of the total O<sub>2</sub> together with the H<sub>2</sub>, a maximum appeared in the CO conversion. This may indicate that it is necessary to optimize the redox state of the catalyst.

CO conversion and oxygen selectivity to CO<sub>2</sub> (not shown) have been studied by moving from the C-1 to the C-4 configuration of the TZFBR, i.e., by changing the fraction of oxygen that is co-fed ( $\xi$ ) at an intermediate point of the catalyst bed (see Fig. 1 for the

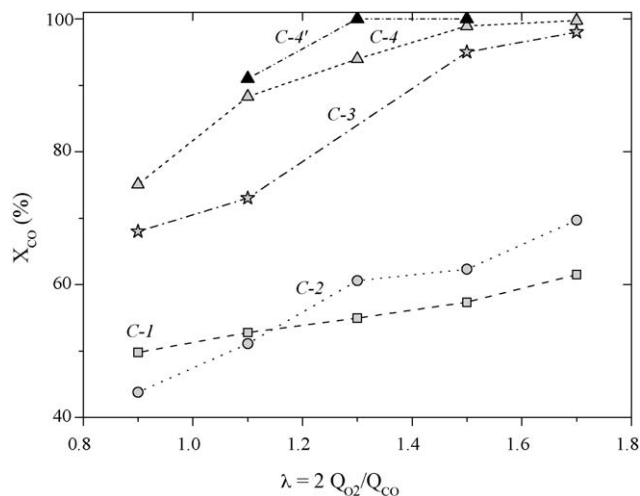


Fig. 6. CO conversion for the PROX reaction as a function of oxygen excess ( $\lambda$ ), for different configurations of the TZFBR.  $T = 80$  °C, 1% CO, 60% H<sub>2</sub>,  $u_{r1} = 4$ ,  $W_{cat} = 40$  g,  $(H_T - h_a)/h_a = 1$  (symbols are experimental data and the lines are guide for eyes).

intermediate configuration between C-1 and C-4). Again, an increase in the amount of co-fed oxygen produces an increase in CO conversion and the oxygen selectivity to CO<sub>2</sub>. The use of a TZFBR allows the oxygen feeding method to be optimized, and thus maximizing the CO conversion and oxygen selectivity to CO<sub>2</sub>. In this case, the maximum CO conversion corresponds to  $\xi = 90\%$ , i.e., a 90% of the total O<sub>2</sub> was co-fed together with the (H<sub>2</sub> + CO) in an intermediate point of the bed and the rest of O<sub>2</sub> was fed in the lower part of the reactor (this configuration of the TZFBR is named C-4'). The influence of the oxygen excess in the C-4' configuration is shown in Fig. 6. The fact of distributing the oxygen fed between the two inlets of the reactor enables the CO conversion to be improved, even for lower values of  $\lambda$ , so that it is possible obtain in the exit flow a CO concentration of less than 10 ppm for  $\lambda = 1.3$ . The oxygen selectivity to CO<sub>2</sub> represented an improvement over other reaction systems where larger values of  $\lambda$  are needed to eliminate completely the CO from a hydrogen-rich flow. For example, Fig. 4 shows that a conventional fluidized bed reactor requires  $\lambda \geq 1.5$  to achieve almost completely CO conversion. These interesting results might be due to a control of the redox state

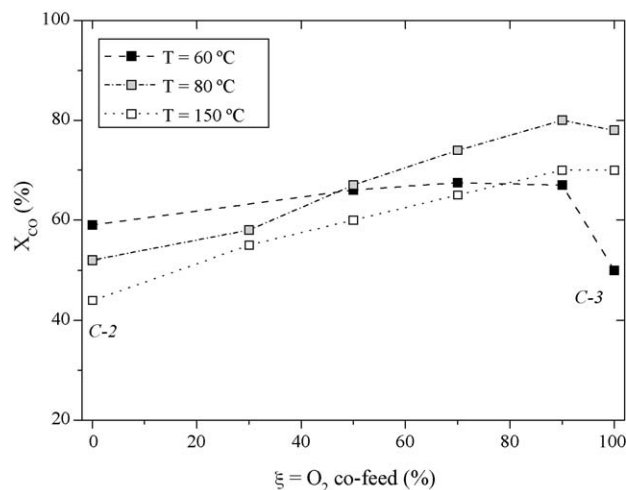
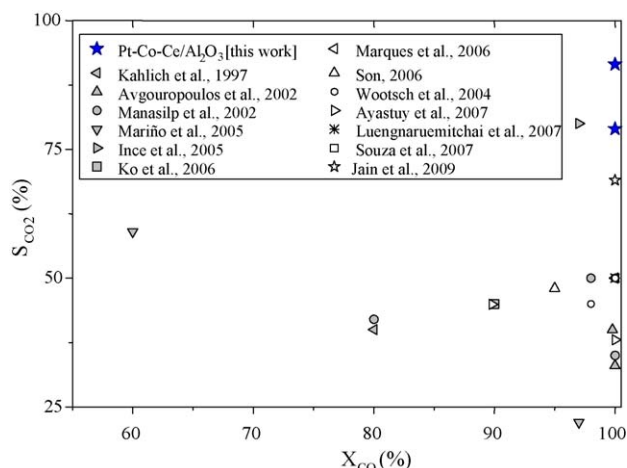


Fig. 7. CO conversion for the PROX reaction as a function of oxygen co-fed with H<sub>2</sub> ( $\xi$ ), for different configurations of the TZFBR. 1% CO, 60% H<sub>2</sub>,  $\lambda = 1.1$ ,  $u_{r1} = 4$ ,  $W_{cat} = 40$  g,  $(H_T - h_a)/h_a = 1$  (symbols are experimental data and the lines are guide for eyes).





**Fig. 8.** Oxygen selectivity to CO<sub>2</sub> as a function of CO conversion. Experiments performed during this work in a TZFBR and FBR and comparison with results in the literature.

of the catalyst, which changes its selectivity in the CO-PROX reaction.

### 3.3. Comparison with results in the literature

Finally, Fig. 8 shows the results obtained in this work with the Pt-Co-Ce/ $\gamma$ -Al<sub>2</sub>O<sub>3</sub> catalyst and the results found in the literature with catalysts based on Pt. Kahlich et al. [21], using a Pt/ $\gamma$ -Al<sub>2</sub>O<sub>3</sub> commercial catalyst, obtained the best results at 225 °C and  $\lambda = 2$ . Avgouropoulos et al. [24] used a Pt/ $\gamma$ -Al<sub>2</sub>O<sub>3</sub> catalyst prepared by incipient wet impregnation, and achieved  $X_{CO} \sim 100\%$  at 160 °C and  $\lambda = 2.5$ . Manasilp and Gulari [17] used a Pt/ $\gamma$ -Al<sub>2</sub>O<sub>3</sub> catalyst, synthesized by the sol-gel method, obtaining the best results at 110 °C with  $\lambda = 2.7$ . Mariño et al. [13] studied a Pt/Ce<sub>x</sub>Zr<sub>y</sub>O<sub>2</sub> catalyst and achieved  $X_{CO} \sim 60\%$  at 100 °C and  $\lambda = 1$ . Woosch et al. [7] tested a Pt/Ce<sub>x</sub>Zr<sub>y</sub>O<sub>2</sub> catalyst and obtained  $X_{CO} = 100\%$  at 150 °C and  $\lambda = 2$ . Ince et al. [9] employed a Pt-Co-Ce/ $\gamma$ -Al<sub>2</sub>O<sub>3</sub> catalyst prepared by the co-impregnation method (catalysts similar to that used in this work) and obtained  $X_{CO} \sim 97\%$  at 90 °C with  $\lambda = 1$ . Ko et al. [26] achieved  $X_{CO} \sim 90\%$  at 177 °C and  $\lambda = 2$  with a Pt-Co/ $\gamma$ -Al<sub>2</sub>O<sub>3</sub> catalyst. Marques et al. [27] with a Pt/Nb<sub>2</sub>O<sub>5</sub> catalyst obtained  $X_{CO} \sim 100\%$  at 90 °C and  $\lambda = 2$ . Son [12], using a Pt-Ce/ $\gamma$ -Al<sub>2</sub>O<sub>3</sub> catalyst, obtained the best results at 200 °C and  $\lambda = 2$ . Ayastuy et al. [11] tested a Pt/MnO<sub>x</sub>/ $\gamma$ -Al<sub>2</sub>O<sub>3</sub> catalyst and achieved the best results at 139 °C and  $\lambda = 2$ . Luengnaruemitchai et al. [22] obtained  $X_{CO} \sim 100\%$  at 200 °C and  $\lambda = 2$  with a Pt supported catalyst over zeolite-A. Souza et al. [28], used a Pt/ $\gamma$ -Al<sub>2</sub>O<sub>3</sub> catalyst and obtained the best results at 150 °C and  $\lambda = 2$ . Jain et al. [29] employed a Pt-Co/ $\gamma$ -Al<sub>2</sub>O<sub>3</sub> catalyst reaching  $X_{CO} \sim 100\%$  at 108 °C and  $\lambda = 1.35$ .

In all these works, fixed bed reactors were used and in some cases catalyst deactivation was reported [9,17,26] due mainly to the formation of carbonates on the catalyst surface that inhibits selective CO oxidation, and that can be eliminated by a treatment of the catalyst. The use of a TZFBR has several advantages over traditional systems used in the CO-PROX reaction, and it allows an effluent to be obtained with a CO concentration of less than 10 ppm with a high selectivity to the selective CO oxidation. This can be obtained by working with just a slight excess of oxygen over that

necessary only to oxidize only the CO present, without catalyst deactivation and operating at temperatures lower than 100 °C.

## 4. Conclusions

Pt-Co-Ce/ $\gamma$ -Al<sub>2</sub>O<sub>3</sub> catalyst was synthesized and tested in the preferential oxidation of CO in a H<sub>2</sub> stream in different fluidized bed reactors. The study of the operating conditions shows a beneficial effect on the CO-PROX reaction at low temperatures and with the presence of CO<sub>2</sub> in the inlet gas. However, water has a negative effect. The oxygen excess has opposing trends in CO conversion and oxygen selectivity to CO<sub>2</sub> and a compromise between them is therefore necessary.

The TZFBR allows the oxidation state of the catalysts to be controlled by changing the point at which reactants are fed. In this work the best results were obtained when feeding 10% of the total oxygen fed at the intermediate point of the reactor, while the rest of the O<sub>2</sub> flow was co-fed at the bottom of the reactor with a H<sub>2</sub> + (1%) CO stream mixed with inert gas. In this case it is possible to achieve a CO conversion  $\sim 100\%$  and oxygen selectivity to CO<sub>2</sub>  $\sim 77\%$ , at 80 °C and  $\lambda = 2Q_{O_2}/Q_{CO} = 1.3$ . The selectivity and conversion obtained with the TZFBR is among the best results reported in the literature using Pt-based catalyst.

## Acknowledgement

The authors thank the DGI (Spain) for financial support for the project CTQ2007-63420/PPQ.

## References

- [1] N. Bion, F. Epron, M. Moreno, F. Mariño, D. Duprez, *Top. Catal.* 51 (2008) 76.
- [2] E.D. Park, D. Lee, H.C. Lee, *Catal. Today* 139 (2009) 280.
- [3] O. Korotkikh, R. Farrauto, *Catal. Today* 62 (2000) 249.
- [4] G.W. Roberts, P. Chin, X. Sun, J.J. Spivey, *Appl. Catal. B* 46 (2003) 601.
- [5] Y. Hasegawa, K. Kusakabe, S. Morooka, J. Membr. Sci. 190 (2001) 1.
- [6] P. Bernardo, C. Algeri, G. Barbieri, E. Drioli, *Catal. Today* 118 (2006) 90.
- [7] A. Woosch, C. Descorme, D. Duprez, *J. Catal.* 225 (2004) 259.
- [8] J. Herguido, M. Menéndez, J. Santamaría, *Catal. Today* 100 (2005) 181.
- [9] T. Ince, G. Uysal, A.N. Akın, R. Yildirim, *Appl. Catal. A* 292 (2005) 171.
- [10] H.L. Liu, M. Lei, S.B. Shao, Z.H. Li, A.Q. Wang, Y.Q. Huang, Z. Tao, *Ch. J. Catal.* 28 (2007) 1077.
- [11] J.L. Ayastuy, M.P. González-Marcos, J.R. González-Velasco, M.A. Gutiérrez-Ortiz, *Appl. Catal. B* 70 (2007) 532.
- [12] I.H. Son, *J. Power Sources* 159 (2006) 1266.
- [13] F. Mariño, C. Descorme, D. Duprez, *Appl. Catal. B* 58 (2005) 175.
- [14] H. Wang, H. Zhu, Z. Qin, F. Liang, G. Wang, J. Wang, *J. Catal.* 264 (2009) 154.
- [15] L.B. Backman, A. Rautiainen, M. Lindblad, A.O.I. Krause, *Appl. Catal. A* 360 (2009) 183.
- [16] J. Choi, B.C. Shin, D.J. Suh, *Catal. Commun.* 9 (2008) 880.
- [17] A. Manasilp, E. Gulari, *Appl. Catal. B* 37 (2002) 17.
- [18] B. Sen, M.A. Vannice, *J. Catal.* 130 (1991) 9.
- [19] C. Kwak, T.J. Park, D.J. Suh, *Chem. Eng. Sci.* 60 (2005) 1211.
- [20] D.H. Kim, M.S. Lim, *Appl. Catal. A* 224 (2002) 27.
- [21] M.J. Kahlich, H.A. Gasteiger, R.J. Behm, *J. Catal.* 171 (1997) 93.
- [22] A. Luengnaruemitchai, M. Nimsuk, P. Naknam, S. Wongkasemjit, S. Osuwan, *Int. J. Hydrog. Energy* 33 (2007) 1.
- [23] R.H. Nibbelke, M.A.J. Campman, J.H.B.J. Hoebink, G.B. Marin, *J. Catal.* 171 (1997) 358.
- [24] G. Avgouropoulos, T. Ioannides, Ch. Papadopolou, J. Batista, S. Hocevar, *Catal. Today* 75 (2002) 157.
- [25] S. Srinivas, E. Gulari, *Catal. Commun.* 7 (2006) 819.
- [26] E.Y. Ko, E.D. Park, K. Won-Seo, H.C. Lee, D. Lee, S. Kim, *Catal. Today* 116 (2006) 377.
- [27] P. Marques, F.P. Nielson, S. Martin, A.G. Donato, M.V. Souza, *J. Power Sources* 158 (2006) 504.
- [28] M.M.V.M. Souza, N.F.P. Ribeiro, M. Schmal, *Int. J. Hydrog. Energy* 32 (2007) 425.
- [29] S.K. Jain, E.M. Crabb, L.E. Smart, D. Thompsett, A.M. Steele, *Appl. Catal. B* 89 (2009) 349.